Relativistic nuclear structure. II. Finite nuclei

H. Müther
Institut für Theoretische Physik, Universität Tübingen, D-7400 Tübingen, West Germany

R. Machleidt
Department of Physics, University of Idaho, Moscow, Idaho 83843

R. Brockmann
Department of Physics, University of Mainz, D-6500 Mainz, West Germany
(Received 27 December 1989)

The Dirac-Brueckner-Hartree-Fock approximation is extended to the calculation of finite nuclei. As an example, the ground-state properties of ^{16}O are studied using modern versions of the one-boson-exchange model for the nucleon-nucleon interaction. The Dirac effect yields a significant increase for the radius of the charge distribution and a moderate gain in binding energy. This improves the agreement with the experimental data considerably, but does not remove the discrepancy between theory and experiment completely.

I. INTRODUCTION

Traditionally, one of the most fundamental goals of nuclear structure physics is to explain the properties of nuclei in terms of the bare interaction between nucleons. Because of the strong nature of the nuclear force and its singular character at short distances, special many-body methods had to be worked out, of which we mention Brueckner theory[1] and the variational approach.[2] Calculations performed for nuclear matter soon revealed that the predictions for the saturation properties based on a variety of nucleon-nucleon (NN) potentials show a systematic behavior: In an energy *versus* density plot the saturation points are located along a band ("Coester band") which does not meet the empirical area.[3–6]

There have been many attempts to overcome this problem. For example, meson and isobar degrees of freedom have been taken into account explicitly in the nuclear many-body problem. Indeed, the inclusion of these subnucleonic degrees of freedom yields modifications in the calculated energy and saturation density, which are nonnegligible. It has been found, however, that these extensions move the calculated saturation point along the Coester band. Therefore, this does not improve the general situation in evaluating saturation properties of nuclear matter.[6]

When Brueckner-type calculations became feasible for finite nuclei, it soon turned out that there are problems analogous to nuclear matter: If the energy of a finite nucleus is predicted about right, the charge radius is substantially too small; on the other hand, when the radius is predicted correctly, the nucleus is underbound by about 50%.[7,8] Again, meson and isobar degrees of freedom did not substantially improve the situation.[9,10]

Recently, a relativistic extension of Brueckner theory was suggested which has become known as the Dirac-Brueckner approach.[11] The new method was inspired by the new development of a relativistic theory for nucleon-nucleus scattering.[12] The basic idea of this approach is to use, for the single-particle motion, a Dirac equation which contains a strong (attractive) scalar and a (repulsive) vector field. The most significant result of this method in nucleon-nucleus scattering is the quantitative fit of spin observables which are only poorly described by the Schrödinger equation.[13]

In nuclear matter the relativistic approach gives rise to a strongly density-dependent repulsive effect, which substantially improves the saturation density. Thus the empirical nuclear matter saturation can be explained quantitatively.[14]

Infinite nuclear matter is a hypothetical system. It is supposed to approximate conditions in the interior of a heavy nucleus. The simple structure of its wave functions (plane waves) makes it quite amenable to numerical solution. However, the final goal of nuclear structure physics is to explain the properties of real nuclei. Miller and Green were the first to study closed-shell nuclei in a relativistic Dirac-Hartree model.[15] Their work was further developed by Brockmann,[16] and Horowitz and Serot,[17] and Serot and Walecka.[18] However, in all of this work (besides Ref. 16) one starts from an effective Lagrangian, the parameters of which are adjusted to the properties of the nuclei. Thus the relation to the fundamental bare NN interaction is lost.

In the Dirac-Brueckner approach for nuclear matter, it has been shown how to base the relativistic approach on the free two-nucleon interaction and thus provide parameter-free predictions for the nuclear many-body system. It is now desirable to pursue for finite nuclei an approach which is equally microscopic and sophisticated as state-of-the-art relativistic nuclear matter calculations. It is the purpose of the present study to start this work. As an example, we choose the closed-shell nucleus ^{16}O. We will apply the meson-theoretic relativistic two-

nucleon potentials presented in an earlier paper[19] (Subsequently denoted by paper I) in which the Dirac-Brueckner formalism and results for nuclear matter are also given.

The results of paper I have shown that nuclear matter saturation can be explained quantitatively in the Dirac-Brueckner-Hartree-Fock approximation. An important question of our present study is if in finite nuclei the relativistic approach will be equally successful. First results of this study have been published in Ref. 20.

In Sec. II we present the formalism we use for the Dirac-Brueckner approach to finite nuclei. Section III contains the results and a discussion. An outlook is given in Sec. IV.

II. DIRAC-BRUECKNER APPROACH FOR FINITE NUCLEI

We start by summarizing the basic formulas used for the Dirac-Bruckner approach to nuclear matter (cf. paper I).

As mentioned in the Introduction, the essential point of the Dirac approach is to use the Dirac equation for the single-particle motion:

$$(\not{p}-M-U)\bar{u}(\mathbf{p},s)=0 \ , \tag{1}$$

with

$$U=U_S+\gamma^0 U_V \ , \tag{2}$$

where U_S is an attractive scalar and U_V (the timelike component of) a repulsive vector field (notation as in Ref. 21). M is the free-nucleon mass.

The solution of Eq. (1) is

$$\tilde{u}(\mathbf{p},s)=\left[\frac{\tilde{E}_p+\tilde{M}}{2\tilde{M}}\right]^{1/2}\begin{pmatrix}1\\ \dfrac{\sigma\cdot p}{\tilde{E}_p+\tilde{M}}\end{pmatrix}\chi_s \ , \tag{3}$$

with

$$\tilde{M}=M+U_S \ , \tag{4}$$

$$\tilde{E}_p=(\tilde{M}^2+\mathbf{p}^2)^{1/2} \ , \tag{5}$$

and χ_s a Pauli spinor. The normalization is

$$\bar{\tilde{u}}(\mathbf{p},s)\tilde{u}(\mathbf{p},s)=1 \ . \tag{6}$$

The relativistic G matrix is obtained as solution of the Bethe-Goldstone type of equation:

$$\tilde{G}(\mathbf{q}',\mathbf{q};\mathbf{P},\tilde{z})=\tilde{V}(\mathbf{q}',\mathbf{q})+\int\frac{d^3k}{(2\pi)^3}\tilde{V}(\mathbf{q}',\mathbf{k})\frac{\tilde{M}^2}{\tilde{E}^2_{P+k}}\times\frac{Q(\mathbf{k},\mathbf{P})}{\tilde{z}-(\tilde{E}_{P+k}+\tilde{E}_{P-k})}\tilde{G}(\mathbf{k},\mathbf{q};\mathbf{P},\tilde{z}) \ , \tag{7}$$

with

$$\tilde{z}=\tilde{E}_{P+q}+\tilde{E}_{P-q} \ , \tag{8}$$

and a Pauli operator $Q(\mathbf{k},\mathbf{P})$, which prevents scattering of nucleons in states below the Fermi surface. $\mathbf{P}$ is one-half the center-of-mass momentum, and $\mathbf{q}$, $\mathbf{k}$, and $\mathbf{q}'$ are the initial, intermediate, and final relative momenta, respectively, of the two particles interacting in nuclear matter. In Eq. (7) we suppressed spin (or helicity) and isospin indices. For $|\mathbf{P}\pm\mathbf{q}|$ and $|\mathbf{P}\pm\mathbf{k}|$ the angle average is used.

It is crucial to note that U_S, U_V, $\tilde{M}$, $\tilde{V}$, and $\tilde{G}$ depend on the density ρ of nuclear matter (which is not indicated explicitly in our notation).

The essential difference to standard Brueckner theory is the use of the potential $\tilde{V}$ in Eq. (7). Indicated by the tilde, this meson-theoretic potential is evaluated by using the spinors [Eq. (3)] instead of the free spinors applied in free-space two-nucleon scattering as well as in conventional ("nonrelativistic") Brueckner theory. For example, the contribution to the potential $\tilde{V}(\mathbf{q}',\mathbf{q})$ from an isoscalar scalar boson exchange (of mass m_s and coupling constant g_s) is

$$\langle \mathbf{q}'s'_m s'_n|\tilde{V}_s|\mathbf{q}s_m s_n\rangle=-g_s^2\frac{\bar{\tilde{u}}(\mathbf{q}',s'_m)\tilde{u}(\mathbf{q},s_m)\bar{\tilde{u}}(-\mathbf{q}',s'_n)\tilde{u}(-\mathbf{q},s_n)}{(\mathbf{q}'-\mathbf{q})^2+m_s^2} \ , \tag{9}$$

where $\mathbf{q}$ ($\mathbf{q}'$) and s_m,s_n (s'_m,s'_n) denote the relative momentum and spin projections, respectively, of the two nucleons before (after) the interaction.

Defining

$$\hat{V}(\mathbf{q}',\mathbf{q};\mathbf{P})=\frac{\tilde{M}}{\tilde{E}_{P+q'}}\tilde{V}(\mathbf{q}',\mathbf{q})\frac{\tilde{M}}{\tilde{E}_{P+q}} \tag{10}$$

and

$$\hat{G}(\mathbf{q}',\mathbf{q};\mathbf{P})=\frac{\tilde{M}}{\tilde{E}_{P+q'}}\tilde{G}(\mathbf{q}',\mathbf{q};\mathbf{P})\frac{\tilde{M}}{\tilde{E}_{P+q}} \ , \tag{11}$$

we can rewrite Eq. (7) in more convenient form:

$$\hat{G}(\mathbf{q}',\mathbf{q};\mathbf{P},\hat{z})=\hat{V}(\mathbf{q}',\mathbf{q};\mathbf{P})+\int\frac{d^3k}{(2\pi)^3}\hat{V}(\mathbf{q}',\mathbf{k}|\mathbf{P})\times\frac{Q(\mathbf{k},\mathbf{P})}{\hat{z}-(\epsilon_{P+k}+\epsilon_{P-k})}\hat{G}(\mathbf{k},\mathbf{q};\mathbf{P},\hat{z}) \ , \tag{12}$$

where we express the energy denominator in terms of the single-particle (s.p.) energies which are defined by

$$\epsilon_m=\frac{\tilde{M}}{\tilde{E}_m}\langle m|\gamma\cdot p_m+M|m\rangle-M+U(m) \tag{13}$$

$$=\tilde{E}_m-M+U_V \ , \tag{14}$$

implying for the starting energy

$$\hat{z}=\epsilon_{P+q}+\epsilon_{P-q} \ . \tag{15}$$

For the s.p. potential

$$U(m)=\frac{\tilde{M}}{\tilde{E}_m}\langle m|U|m\rangle=\frac{\tilde{M}}{\tilde{E}_m}\langle m|U_S+\gamma^0 U_V|m\rangle$$
$$=\frac{\tilde{M}}{\tilde{E}_m}U_S+U_V\ , \tag{16}$$

a Brueckner-Hartree-Fock (BHF) definition is used:

$$U(m)=\mathrm{Re}\sum_{n\le k_F}\langle mn|\hat{G}(\hat{z})|mn-nm\rangle\ , \tag{17}$$

from which the constants U_S and U_V are determined in a self-consistent way.

Finally, the energy per particle in nuclear matter is obtained in lowest order by

$$\frac{\mathcal{E}}{A}=\frac{1}{A}\sum_{m\le k_F}\frac{\tilde{M}}{\tilde{E}_m}\langle m|\gamma\cdot p_m+M|m\rangle-M$$
$$+\frac{1}{2A}\sum_{m,n\le k_F}\langle mn|\hat{G}(\hat{z})|mn-nm\rangle. \tag{18}$$

In Eqs. (17) and (18) it is used:

$$\hat{z}=\epsilon_m+\epsilon_n\ . \tag{19}$$

This summarizes the Dirac-Brueckner-Hartree-Fock (DBHF) formalism for nuclear matter.

We now discuss our approach to finite nuclei. The Brueckner equation, which is given explicitly for the case of plane-wave states in Eq. (12), is solved directly for the nucleus under consideration. The techniques which are applied to solve the BHF equations for finite nuclei in a self-consistent way are identical to those described in Ref. 9. Also, here we use a basis of harmonic-oscillator states to expand the self-consistent BHF states and consider an appropriate Pauli projector Q in the Bethe-Goldstone equation for finite nuclei (see Ref. 9 for details).

In the relativistic extension of the BHF approach, one has to account for the fact that the Dirac spinors are modified in the nuclear medium, which yields a density dependence for the matrix elements of the meson-exchange interaction $\hat{V}$ [Eq. (10)]. In the present approach, we determine this medium dependence of the interaction $\hat{V}$ from the calculations in nuclear matter using an effective-density approximation: For each pair of interacting nucleons we evaluate an average density

$$\rho_{mn}=\sqrt{\rho_m\rho_n}\ , \tag{20}$$

with

$$\rho_m^{1/3}=\int d^3r\,\phi_m^*(\mathbf{r})\phi_m(\mathbf{r})\rho^{1/3}(\mathbf{r})\ , \tag{21}$$

where $\phi_m(\mathbf{r})$ is the BHF s.p. wave function and $\rho(\mathbf{r})$ the density of ^{16}O as obtained from the BHF Slater determinant. The density dependence of the interaction $\hat{V}$ introduces an additional self-consistency requirement since the BHF wave function ϕ_m depends on the interaction $\hat{V}$ and vice versa. As usual, this self-consistency is achieved in an iterative scheme.

Formally, in the finite nucleus calculation, we also use Eqs. (13), (17), and (18). Note, however, that the states m and n now represent s.p. states of ^{16}O expanded in a harmonic-oscillator basis. The medium dependence of the Dirac spinors is also reflected in the first term on the right-hand side (rhs) of Eq. (13)—the "kinetic energy"—which in more explicit form reads

$$t_m=\frac{M\tilde{M}+\mathbf{p}_m^2}{\tilde{E}_m}-M\ . \tag{22}$$

To be consistent with the treatment of the medium dependence of the interaction, we apply the effective-density approach for the calculation of the kinetic energy. This means that in calculating the kinetic energy for a nucleon in the BHF state m, we use an effective mass $\tilde{M}$, which is obtained from nuclear matter of density ρ_m [Eq. (21)]. Since we have to evaluate the matrix elements of the operator t_m in a basis of harmonic-oscillator states (used to represent the BHF states), we expand t_m in powers of $\mathbf{p}_m^2/2m$:

$$t_m=\left[\frac{\mathbf{p}_m^2}{2M}\right]\frac{2M\tilde{M}-M^2}{\tilde{M}^2}+\left[\frac{\mathbf{p}_m^2}{2M}\right]^2\frac{3M^3-4M^2\tilde{M}}{2\tilde{M}^4}$$
$$+\left[\frac{\mathbf{p}_m^2}{2M}\right]^3\frac{6M^3\tilde{M}-5M^4}{2\tilde{M}^6}+\cdots\ . \tag{23}$$

This expansion is used in Eqs. (13) and (18). As we will discuss later, the expansion up to third order has proven to be sufficiently accurate for the examples under consideration.

III. RESULTS AND DISCUSSION

To study the effects of the Dirac phenomenology, we consider three relativistic one-boson-exchange potentials (OBEP) which were presented in paper I where also the results for nuclear matter were given. These potentials differ essentially in the strength of the tensor force. A measure for this strength is the predicted D-state probability of the deuteron which is 4.5%, 5.1%, and 5.5% for potentials A, B, and C, respectively. Depending on the strength of the tensor force, the potentials lead to rather different predictions for the energy of a many-nucleon system.

This can be seen from the results of conventional BHF calculations displayed in Fig. 1 In this figure we show the calculated energy per nucleon and the inverse value of the radius of the charge distribution for the ground state of ^{16}O. Note that we call a calculation "conventional" or "nonrelativistic" in which the Dirac effects are ignored: The relativistic potential $\hat{V}$ [Eq. (10)] and the kinetic energy [Eq. (22)] are used as calculated in the vacuum (i.e., with $\tilde{M}=M$).

As in nuclear matter, we obtain much more binding energy using the weak tensor force potential A as compared to B or C, which have stronger tensor force components. This behavior is easily understood in the following way: A strong tensor force yields large attractive contributions to the scattering matrix T because of terms of second and higher order in the potential iterated in the Lippmann-Schwinger equation. Since all potentials were adjusted to fit the empirical phase shifts, a weak tensor

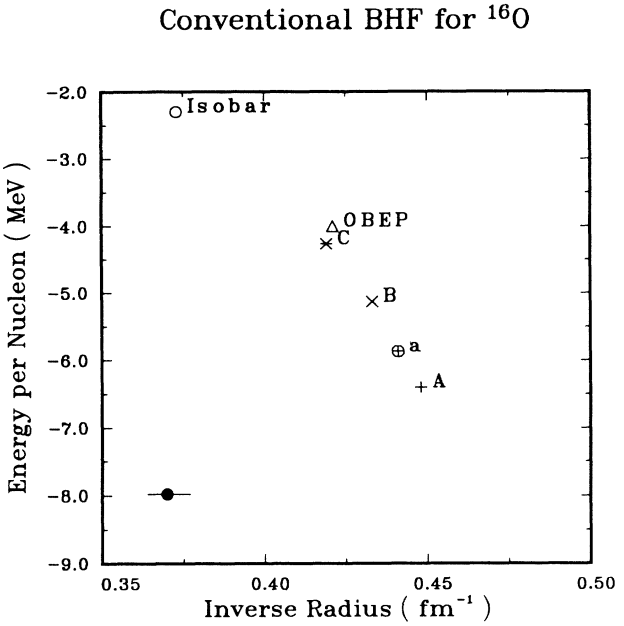

FIG. 1. Conventional BHF calculations for ^{16}O. Results are plotted for the calculated energy per nucleon, $\mathcal{E}/A$, vs the inverse charge radius applying potentials *A*, *B*, and *C*, as denoted. The point marked by *a* is obtained from a BHF calculation using the nonrelativistic approximation for the kinetic energy (applying potential *A*). For comparison we also show results from former nonrelativistic calculations using an OBE potential ("OBEP") (Ref. 7) and a model which includes effects due to virtual Δ-isobar excitations ("Isobar") (Ref. 9). The error bar denotes the empirical point.

component must be accompanied by a more attractive central component to give the same attraction in the vacuum. In the Bethe-Goldstone equation [Eq. (12)], the Pauli operator as well as the different s.p. energies in the energy denominator reduce the contributions of higher order as compared to the corresponding terms in the Lippmann-Schwinger equation. This loss of attraction is larger for a potential with a stronger tensor force, leading to less binding. Moreover, a system of nucleons (interacting by forces of short range) that is more bound tends to have a smaller radius. These two aspects essentially explain the "Coester band" for the ground state of ^{16}O established by the BHF results using potentials *A*, *B*, and *C*.

Our present results, ignoring the Dirac effects, fit into the "Coester band" obtained in earlier calculations. As examples, we display in Fig. 1 the BHF result from an older OBEP application ("OBEP") (Ref. 7) and from a calculation which takes virtual Δ-isobar excitation into account ("Isobar").[9] Again, none of these results fit the empirical point.

To demonstrate the effect of the relativistic treatment of the kinetic energy, we show for the case of potential *A* the BHF result with the expression for the kinetic energy replaced by the nonrelativistic approximation, which is the first term in the expansion [Eq. (23)]. This result is denoted by the small letter *a* in Fig. 1. The higher-order terms in the expansion [Eq. (23)] reduce the repulsive effect of the kinetic energy. Therefore, the binding energy obtained in the BHF calculation with the relativistic treatment of the kinetic energy is larger than for the nonrelativistic approach. This gain in binding energy is accompanied by a reduction of the calculated radius, and thus both results are located on the "Coester band."

In Table I some results of conventional (nonrelativistic) *renormalized* BHF calculations are listed. The renormalized BHF approach is a slight modification of the BHF approximation in solving the many-body problem. In the renormalized BHF approach the single-particle potential U is defined by

$$\langle a|U|b\rangle = \sum_{n\le F} \langle an|\hat{G}(\hat{z})|bn-nb\rangle P_n \ , \tag{24}$$

with an occupation probability

$$P_n = \left[1-\sum_{m\le F}\left\langle nm\left|\frac{\partial\hat{G}}{\partial\hat{z}}\right|mn-nm\right\rangle P_m\right]^{-1} . \tag{25}$$

These occupation probabilities take into account that the two-body correlations lead to a depletion of the Fermi sea. The deviation of P_n from one is related to the wound integral and, therefore, also a measure for the amount of correlations. Occupation probabilities for the proton-hole states in ^{16}O are listed in Table I. As to be expected, the deviation from one is largest for the potential *C*, which has the strongest tensor components among the potentials under consideration. It should be noted, however, that even the occupation probabilities obtained for *C* are larger than those obtained for old phenomenological potentials like Reid soft core[7] ($P_n \approx 0.88$) which typically have a stronger tensor component. Since the occupation probabilities are close to 1, the modifications of the renormalized BHF as compared to BHF are small.

TABLE I. Ground-state properties of ^{16}O in a nonrelativistic renormalized BHF calculation. Given are results for the single-particle energies and occupation probabilities of the occupied proton states, the total energy per nucleon, $\mathcal{E}/A$, and the radius of the charge distribution, r_c, accounting for the finite size of the proton and correcting for center-of-mass motion. The last column displays the experimental data. Energies are in units of MeV, radii in fm. Results are given for the potentials *C*, *B*, and *A*, including the effects of the Coulomb interaction between protons.

	C	*B*	*A*	Experiment
$s_{1/2}$	−39.73	−44.37	−50.46	−40±8
	0.906	0.907	0.907	
$p_{3/2}$	−16.98	−19.49	−22.89	−18.4
	0.926	0.930	0.935	
$p_{1/2}$	−11.64	−13.24	−15.44	−12.1
	0.924	0.929	0.935	
$\mathcal{E}/A$	−4.49	−5.35	−6.56	−7.98
r_c	2.465	2.380	2.291	2.70±0.05

Therefore, the improvements of the BHF approach as compared to the BHF results are too small to get close to the empirical point. As an example, we mention that for potential A the calculated binding energy per nucleon is shifted from 6.4 MeV (radius 2.23 fm) in the BHF approximation to 6.56 MeV (2.29 fm) in the renormalized BHF approach.

The extended BHF definition for the single-particle potential [Eq. (24)] can also be understood to include rearrangement terms in the single-particle potential.[22] Therefore, one may consider the single-particle energies resulting from the renormalized BHF approach as a first approximation to a prediction for separation energies of single nucleons. Having this in mind, Table I demonstrates another problem of conventional BHF or renormalized BHF calculations. Considering, e.g., the results obtained with potential A, one finds that the calculated single-particle energies show more attraction than the empirical ones. The total binding energy, however, is still below the empirical value. For potentials B and C the results for the single-particle energies get closer to the experimental data, while the result for the binding energy gets worse.

In the BHF approximation the total energy $\mathcal{E}$ and the single-particle energies ϵ_m are related by

$$\mathcal{E}=\sum_{m\le F}\frac{\epsilon_m+t_m}{2}\ , \tag{26}$$

where ϵ_m (t_m) stands for the single-particle (kinetic) energy of a nucleon in the self-consistent single-particle state M. This relation is approximately also valid in the renormalized BHF approach. To obtain a more attractive total energy $\mathcal{E}$ without lowering the values for the single-particle energies, the relation Eq. (26) must be broken. This could be achieved by going beyond the BHF approximation and including terms of higher order, or by a mechanism which reduces the repulsion due to the kinetic energy. The kinetic energy is reduced when the radius of the nucleus becomes larger. Thus the problem of the mismatch in single-particle energies and total energy and the problem of obtaining too small a radius are related.

In order to study the effects of the change of the Dirac spinors in the nuclear medium on the calculated ground-state properties of ^{16}O, we consider, as a next step, the interaction $\hat{V}$ between Dirac spinors of nuclear matter at a given density ρ_0 using the effective mass $\tilde{M}$ determined for nuclear matter at that density ρ_0. This means that we perform a Dirac BHF calculation as outlined in Sec. II, but instead of determining the densities ρ_{mn} [Eq. (20)] and the effective mass $\tilde{M}$ in a self-consistent way, we use $\tilde{M}$ at ρ_0. Results of such calculations are displayed in Fig. 2 as a function of ρ_0. As an example, we consider potential C. The results for the other potentials are very similar.

It can be observed from Fig. 2 that the single-particle energy for a nucleon in the lowest $s_{1/2}$ state gets less attractive with increasing density ρ_0. This is due to the fact that the change of the Dirac spinors in the nuclear medium yields less attractive matrix elements for $\hat{V}$ with increasing density. As discussed in paper I, this can essentially be attributed to a supression of the (attractive) one-sigma exchange. The reduction of the attractive components in $\hat{V}$ also yields an increase of the radius calculated for ^{16}O with increasing ρ_0. Note, however, that the dependence of the single-particle energy and the radius on ρ_0 becomes flat at higher densities (the highest density displayed in this figure, $\rho_0=0.15$ fm^{-3}, is about equal to the saturation density of nuclear matter). This is due to the fact that the kinetic energy decreases with increasing ρ_0 and counterbalances the reduced attraction from the interaction. There are two mechanisms which are responsible for this decrease of the kinetic energy: First, the decrease of $\tilde{M}$ with ρ_0 and, second, the increase of the radius for ^{16}O. While the first mechanism also takes place in nuclear matter, the second effect is a typical feature of finite systems. The decrease of the kinetic energy with an increase of ρ_0 has an even larger effect on the total energy [see Eq. (26)]; the binding energy increases with increasing ρ_0. This is different from nuclear matter where the Dirac effects lead to a decrease of the binding energy at all densities.

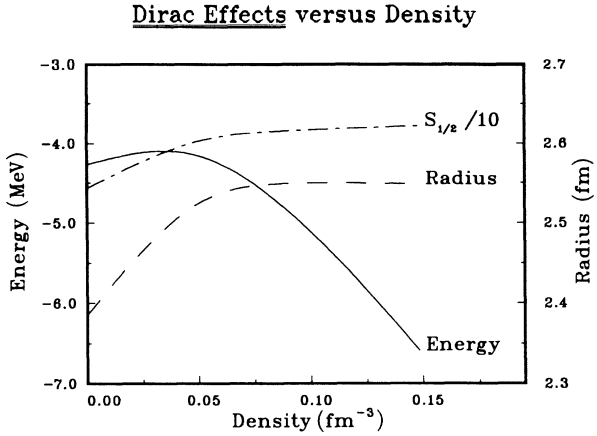

FIG. 2. Effect of Dirac spinors, determined for nuclear matter at various densities, on properties of ^{16}O. As a function of the density parameter ρ_0, used for the effective mass $\tilde{M}$ and $\hat{V}$, results from Dirac-BHF calculations are given for the total energy per nucleon (solid line), the single-particle energy of a proton in the lowest $s_{1/2}$ state (divided by 10 dot-dashed line), and the radius of the charge distribution (dashed line; see scale on the right side of the figure).

After we have discussed the influence of the change of Dirac spinors in the medium as a function of ρ_0, we now turn to calculations in which this density is determined in a self-consistent way. As outlined in Sec. II, we determine a self-consistent value for the density parameter ρ_{mn} individually for each pair of interacting nucleons [see Eqs. (20) and (21)]. This density is used in the evaluation of $\hat{V}$. Also the effective mass, which is needed in calculating the kinetic energy, is determined for each single-particle state separately. In order to test the sensitivity of the results on this choice for ρ and $\tilde{M}$, we have also performed calculations in which we have determined one global value for these quantities obtained by averaging over all states.

TABLE II. Ground-state properties of ^{16}O in a renormalized Dirac-BHF calculation. Results are presented for the potentials *C*, *B*, and *A* using the effective-density approach for the treatment of Dirac effects with densities ρ_{mn} different for each pair of interacting nucleons as described in Eqs. (20) and (21). The column labeled "global" shows results obtained by replacing the individual densities ρ_{mn} by the average density of all states (using potential *A*). For further details see Table I.

	C	*B*	*A*	Global	Experiment
$s_{1/2}$	−34.31 0.919	−39.15 0.921	−44.25 0.924	−42.53 0.926	−40±8
$p_{3/2}$	−15.34 0.933	−17.09 0.937	−19.77 0.942	−20.18 0.942	−18.4
$p_{1/1}$	−9.44 0.928	−9.94 0.932	−11.16 0.937	−11.88 0.937	−12.1
$\mathcal{E}/A$	−4.95	−5.84	−7.08	−6.97	−7.98
r_c	2.610	2.534	2.450	2.447	2.70±0.05

A comparison of the individual and global self-consistency requirements is made in Table II, where for a renormalized Dirac-BHF calculation we compare the two choices using potential *A*. The differences for the calculated total energy per nucleon and the radius of the charge distribution (0.1 MeV and 0.003 fm, respectively) are negligible. The differences are slightly larger for the calculated single-particle energies, and it can be observed that the spectrum of single-particle energies obtained from the global approach is slightly more compressed. However, the differences are small enough to conclude that the dependence of the results on how the effective densities are determined is not very significant.

Another approximation, which has been used, is the truncation of the expansion of the operator for the relativistic kinetic energy [Eq. (23)]. For the results listed in the tables and figures, we have included all terms up to third order in $p^2/2M$. If we only include terms up to second order, the resulting energy is typically changed by 0.1 MeV per nucleon and the radius by 0.01 fm. Thus the expansion seems to converge rather well, and the difference between the third-order approximation and the complete expansion should be even smaller.

Results for the ground-state properties of ^{16}O, calculated in the BHF approximation with and without inclusion of the effects of the Dirac phenomenology, are displayed in the energy *versus* inverse radius plot of Fig. 3. The results for the conventional BHF calculations are indicated by the crosses, and those for the relativistic approach are given by the circles. For each potential the results are connected by a straight line. It is seen that for all cases under consideration, the inclusion of the Dirac effects increases both the calculated energy and the radius of the charge distribution, considerably (see discussion above). Thus the predictions by the theory are moved towards the empirical point. The relativistic effects seem to be slightly larger for potential *A* as compared to *B* and *C*.

This may be due to the fact that the nuclear densities which occur in calculations using potential *A* are slightly larger than those for the other two potentials. Including the relativistic features in the BHF approach, a new Coester band is formed, which is closer to experiment. However, the Dirac effects are not large enough to bring the theoretical predictions to a complete agreement with the empirical point; in fact, they make up for only about half of the original discrepancy in conventional BHF calculations.

Some results for renormalized Dirac-BHF calculations are listed in Table II. We find that the Dirac effects not only improve the results for the total energy and radius, but also yield a much better simultaneous description of

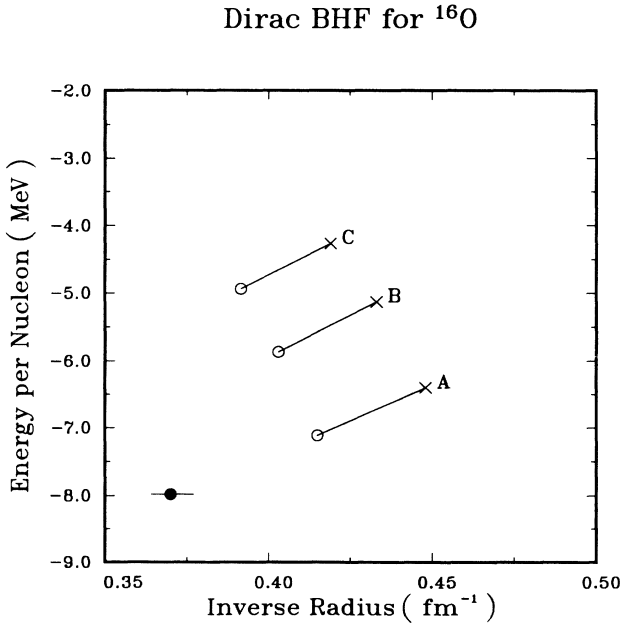

FIG. 3. Relativistic and nonrelativistic BHF calculations for ^{16}O. Using potentials *A*, *B*, and *C*, results of conventional BHF calculations (crosses) and Dirac-BHF calculations (circles) are displayed in an energy versus inverse radius plot. See also Fig. 1

single-particle energies and total energy. For the case of the potential *A*, the single-particle energies are in reasonable agreement with the empirical results, and the total energy is only off by 1 MeV per nucleon.

It has been a long-standing problem in microscopic nuclear structure calculations to obtain spin-orbit splitting in the single-particle energies sufficiently large to agree with the empirical values. Our results listed in Table II for potential *A* are even overestimating the energy difference between $p_{3/2}$ and $p_{1/2}$ states. This success is partly due to the inclusion of relativistic features in the BHF calculation. Note, however, that in our calculations the nonrelativistic results listed in Table I are already quite close to the empirical values. This may be attributed to the modern *NN* interactions fitting recent two-nucleon data used in the present study.

The occupation probabilities are getting slightly larger when relativistic features are taken into account (compare Tables I and II). This may be an indication for the fact that iterated one-pion-exchange contributions, which are to a large extent responsible for the deviation of the occupation probabilities from 1, are reduced with decreasing effective mass for the nucleon, if a pseudovector coupling is used for the pion. This effect is taken into account only for the relativistic approach.

IV. SUMMARY AND OUTLOOK

In the present paper we have studied the effects of the Dirac phenomenology on the calculation of ground-state properties of finite nuclei (^{16}O) within the framework of the Brueckner-Hartree-Fock (BHF) and renormalized BHF approach considering three modern versions of relativistic OBE potentials which fit the *NN* phase shifts. The self-consistency problem of the BHF equations has been solved directly for the finite nucleus. The density dependence of the interaction and the kinetic energy, which is due to the change of the Dirac spinors in the nuclear medium, is deduced from the studies in nuclear matter and treated in an effective-density approximation. The final results are not very sensitive to the details of this effective density approach.

The effects of the Dirac phenomenology yield an increase of the calculated binding energy per nucleon and the radius of the charge distribution. This moves the results off the "Coester band" of conventional BHF calculations and closer to the empirical value. The remaining discrepancy is about one-half of the failure of the original nonrelativistic BHF approach. A substantial improvement can also be seen in the simultaneous description of single-particle energies and the total energy. The degrees of freedom, which are due to the finite size of the system, lead to self-consistency effects which are quite different from those in nuclear matter.

It must be pointed out, however, that although the Dirac-BHF approach yields considerable improvements in predicting ground-state properties of finite nuclei, it is not able to provide a completely satisfactory agreement with the data. Thus one may raise several questions: Why does the approach, which is successful in describing the ground-state properties of nuclear matter starting from a realistic *NN* interaction, not work equally well in finite nuclei? Can one move the remaining discrepancies by improving the effective-density approximation for the Dirac effects? This will be studied. Since, however, the results were rather insensitive to the details of this approach, we do not expect very large corrections. Also, an extension of the conventional many-body theory, beyond BHF, could remove the discrepancy. Typically, the effects of many-body correlations increase with the density of the system under considerations. Therefore, such improvements should affect the saturation properties of nuclear matter much more than those of ^{16}O, which has an average density of only one-half of the nuclear matter density. Thus there is not much hope that the solution of the remaining problems may come from these aspects.

Calculations in finite systems are much more sensitive to the range of the interaction between the constituents than calculations in infinite systems. There are several indications (see, e.g., Ref. 23) that a nuclear medium does not only lead to a decrease of the effective masses of the nucleons, but also reduces the effective masses of the mesons, especially the σ meson. This will increase the range of the attractive component of the *NN* interaction, which should lead to larger radii and more binding energy. This could be a clue for solving the remaining problems in calculating the gross features of finite nuclei in a microscopic way.

ACKNOWLEDGMENTS

This work was supported in part by the U.S. National Science Foundation under Grant No. PHY-8911040 and the NSF San Diego Supercomputer Center. Furthermore, we acknowledge partial support by the West German Bundesministerium für Forschung und Technologie (06 Tü 714) and a NATO Grant (0147/89).

[1]B. D. Day, Rev. Mod. Phys. **39**, 719 (1967).
[2]B. D. Day, Rev. Mod. Phys. **50**, 495 (1978); V. R. Pandharipande and R. B. Wiringa, *ibid.* **51**, 821 (1979).
[3]F. Coester, S. Cohen, B. D. Day, and C. M. Vincent, Phys. Rev. C **1**, 769 (1970).
[4]B. D. Day, Comments Nucl. Part. Phys. **11**, 115 (1983).
[5]B. D. Day and R. B. Wiringa, Phys. Rev. C **32**, 1057 (1985).
[6]R. Machleidt, Adv. Nucl. Phys. **19**, 189 (1989).
[7]R. Machleidt, H. Müther, and A. Faessler, Nucl. Phys. **A241**, 18 (1975).
[8]H. Kümmel, K. H. Lührmann, and J. G. Zabolitzky, Phys. Rep. **36**, 1 (1978).
[9]M. R. Anastasio, A. Faessler, H. Müther, H. Holinde, and R. Machleidt, Phys. Rev. C **18**, 2416 (1978).
[10]H. Müther, Prog. Part. Nucl. Phys. **14**, 123 (1984).
[11]M. R. Anastasio, L. S. Celenza, W. S. Pong, and C. M. Shakin, Phys. Rep. **100**, 327 (1983).
[12]L. G. Arnold, B. C. Clark, and R. L. Mercer, Phys. Rev. C **19**, 917 (1979).
[13]S. J. Wallace, Annu. Rev. Nucl. Part. Sci. **37**, 267 (1987).

[14]R. Brockmann and R. Machleidt, Phys. Lett. **149B**, 283 (1984).
[15]L. D. Miller and A. E. S. Green, Phys. Rev. C **5**, 241 (1972).
[16]R. Brockmann, Phys. Rev. C **18**, 1510 (1978).
[17]C. J. Horowitz and B. D. Serot, Nucl. Phys. **A368**, 503 (1981).
[18]B. D. Serot and J. D. Walecka, Adv. Nucl. Phys. **16**, 1 (1986).
[19]R. Brockmann and R. Machleidt, Phys. Rev. C **42**, 1965 (1990), the preceding paper.
[20]H. Müther, R. Machleidt, and R. Brockmann, Phys. Lett. B **202**, 483 (1988).
[21]J. D. Bjorken and S. D. Drell, *Relativistic Quantum Mechanics* (McGraw-Hill, New York, 1964).
[22]H. Müther, A. Faessler, and K. Goeke, Nucl. Phys. **A215**, 213 (1973).
[23]G. E. Brown, H. Müther, and M. Prakash, Nucl. Phys. **A506**, 565 (1990).